



Supplement of

Driving factors of aerosol acidity: a new hierarchical quantitative analysis framework and its application in Changzhou, China

Xiaolin Duan et al.

Correspondence to: Guangjie Zheng (zgj123@mail.tsinghua.edu.cn) and Chuchu Chen (chence3@mail.tsinghua.edu.cn)

The copyright of individual parts of the supplement might differ from the article licence.

Supplementary Text

S1. Detailed description of decomposing parameters into 4 time series components

20 The decomposition process consists of the following main steps: linear-fitting of the long-term trends, one-term Fourier curve fitting of seasonal and diurnal variations, and extraction of random residues. For parameter p , this process is expressed as Eq. S1a-d:

$$p_{yr} = a_1 * t + b_1 \quad (S1a)$$

$$p_{seas} = a_2 + b_2 * \sin(\omega_1 * t) + c_1 * \cos(\omega_1 * t) \quad (S1b)$$

25
$$p_{day} = a_3 + b_3 * \sin(\omega_2 * t) + c_2 * \cos(\omega_2 * t) \quad (S1c)$$

$$p_{res} = p - p_{yr} - p_{seas} - p_{day} \quad (S1d)$$

where p , p_{yr} , p_{seas} , p_{day} and p_{res} are the values of actual observed, long-term trend, seasonal variation, diurnal cycle and residues, respectively. The t is the time, and a_i , b_i and c_i are the coefficients of fitted curves during the corresponding time series, respectively. ω_1 and ω_2 are $2\pi/365$ days⁻¹ and $2\pi/24$ hours⁻¹,
30 respectively, to fixed the cycle period of Fourier curve as 1 year and 1 day in fitting the seasonal and diurnal variations.

S2. Detailed descriptions of quantitative analysis of each factor based on ISM and time series analysis

Here we adopted a bottom-up method to quantify the time series components of upper-level factors in
35 the ISM model and its driving factors. That is, based on the decomposition of time series analysis, each input parameter p in ISORROPIA v2.3 is subdivided into 4 time series components. The underlying principle of such decompositions is that most influencing factors of aerosol acidity, such as temperature and emissions, are influenced by long-term variations, periodical variations (i.e., seasonally and diurnally) and random fluctuations (Anderson, 2011; Wei, 2013). For example, temperature can be decomposed
40 into long-term trend (T_{yr}), seasonal variations (T_{seas}), diurnal cycles (T_{day}) and residuals (T_{res}), respectively. Then, the corresponding components are used in ISORROPIA calculations to achieve the quantitative assessment of factors affecting pH at corresponding time series.

Taking factors contribution to X_{gp} seasonal variations for example, there are two parts for calculation:

$\partial X_{gp}|_{seas}$ and factor x_i contribution to $\partial X_{gp}|_{seas}$ (i.e., $\partial X_{gp}/\partial x_i|_{seas}$)

45 **(1) Calculation of X_{gp} seasonal variations $\partial X_{gp}|_{seas}$**

In the seasonal variation's scenario, values of input parameter p is (Eq. S2a)

$$p = \bar{p} + p_{seas} \quad (S2a)$$

where \bar{p} is the average values of p and p_{seas} is the decomposed seasonal values in time series analysis. Based on Eq. S2a, ISORROPIA v2.3 and Eq.2d in main text, $X_{gp|calc}$ is obtained. Then $\partial X_{gp}|_{seas}$ is calculate
50 as (Eq. S2b)

$$\partial X_{gp}|_{seas} = X_{gp|calc} - \overline{X_{gp}} \quad (S2b)$$

where $\overline{X_{gp}}$ is obtained based on average values of input parameters.

(2) Calculation of factor contributions $\partial X_{gp}/\partial x_i|_{seas}$

With the ISM in main text, main influence factors of X_{gp} are temperature and relative abundance of
55 alkaline to acidic substances (C_t/A_t). These factors variations contribute to $\partial X_{gp}|_{seas}$ are obtained as follows:

$$\partial X_{gp}/\partial T|_{seas} = X_{gp}(T_{seas} + \bar{T}, \overline{C_t/A_t}) - X_{gp}(\bar{T}, \overline{C_t/A_t}) \quad (S2c)$$

$$\partial X_{gp}/\partial(C_t/A_t)|_{seas} = \partial X_{gp}|_{seas} - \partial X_{gp}/\partial T|_{seas} \quad (S2d)$$

where T_{seas} is the decomposed seasonal variations of temperature. $\overline{C_t/A_t}$ is obtained based on the base-
60 line values of input parameters. As for C_t/A_t , its contribution to $\partial X_{gp}|_{seas}$ is the differences between $\partial X_{gp}|_{seas}$ and $\partial X_{gp}/\partial T|_{seas}$ (Eq. S2d), and this approach is also applicable to contribution of $PM_{2.5}$ to AWC, temperature to c_{ni} and chemical profiles to f_{NO_3} . Then quantitative contributions of middle-level influencing factors for $\partial X_{gp}|_{seas}$ are obtained. The contributions of middle-level factors to top-level influencing factors are calculated using a similar process for each time series component. Ultimately, the
65 quantitative contributions of chemical profiles, RH, temperature and $PM_{2.5}$ concentrations to pH are obtained for each time series component as well as for the entire observation period.

S3. Detailed description of variation contribution quantification

To illustrate the one-at-a-time sensitivity analysis method, driving factor analysis of c_{ni} variations is taken
for example here. The c_{ni} depends mainly on RH, temperature T and the fraction of NO_3^- in anions (f_{NO_3})
70 (Zheng et al., 2022). Based on the calculation method of previous study and ISORROPIA model, these influencing factors contributions to c_{ni} variations can be quantitative analyzed by Eqs.S3 as:

$$\partial c_{\text{ni}}/\partial_{RH} = c_{\text{ni}}(RH, \bar{T}, \overline{f_{\text{NO}_3^-}}) - c_{\text{ni}}(\overline{RH}, \bar{T}, \overline{f_{\text{NO}_3^-}}) \quad (\text{S3a})$$

$$\partial c_{\text{ni}}/\partial_{f_{\text{NO}_3^-}} = c_{\text{ni}}(\overline{RH}, \bar{T}, f_{\text{NO}_3^-}) - c_{\text{ni}}(\overline{RH}, \bar{T}, \overline{f_{\text{NO}_3^-}}) \quad (\text{S3b})$$

$$\partial c_{\text{ni}}/\partial_T = \partial c_{\text{ni}} - \partial c_{\text{ni}}/\partial_{f_{\text{NO}_3^-}} - \partial c_{\text{ni}}/\partial_{RH} \quad (\text{S3c})$$

75 Where \bar{X} and X are the average values and decomposed values of variable X , respectively, and more detailed calculations are described in SI Text S2.

S4. Detailed descriptions of hierarchical relationship between influencing factors for c_{ni} and X_{gp} in ISM

80 The c_{ni} causes direct effects on aerosol pH (Top-level). As shown in Eq. 2c, c_{ni} is the ratio of activity coefficients, which firstly depends on RH and Temperature (middle-level). The NO_3^- and SO_4^{2-} are the main anions paired with H^+ or NH_4^+ in ammonia-buffered ambient aerosols, and it has been shown that c_{ni} differs between sulfate- and nitrate-dominated aerosols (Zheng et al., 2022). The c_{ni} at a given RH and temperature therefore depends on the anion profiles, which can be expressed as the fraction of NO_3^- in anions (aq), i.e., $f_{\text{NO}_3^-}$ (middle-level) (Zheng et al., 2022). The $f_{\text{NO}_3^-}$ is further sensitive to temperature, 85 which influences the gas-particle partitioning of volatility of semi-volatile species like ammonium nitrate, and chemical profiles (middle-level). Meteorological parameters and chemical profiles are fundamentally related to synoptic conditions and emissions (bottom-level).

X_{gp} also directly affects aerosol pH (top-level), and its variation is influenced by temperature and chemical profiles (middle-level) (Zheng et al., 2024). Similar with $\text{p}K_{\text{a}}^*$ and c_{ni} , the root of these 90 variations is synoptic conditions and emissions (bottom-level).

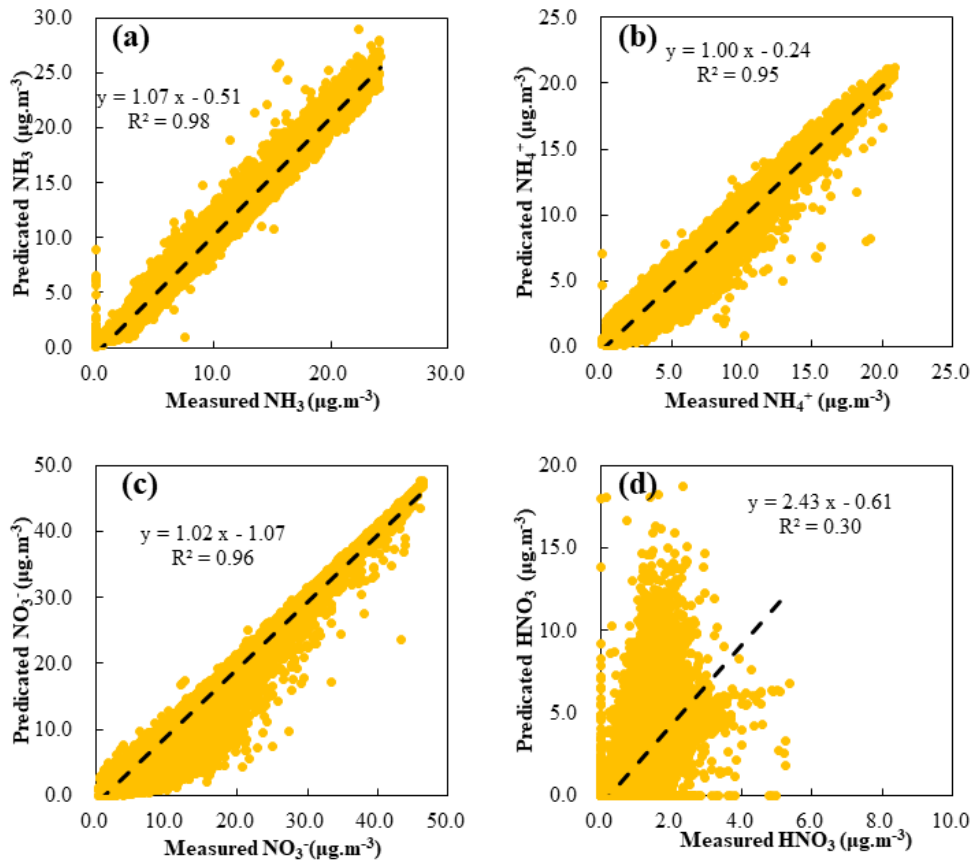
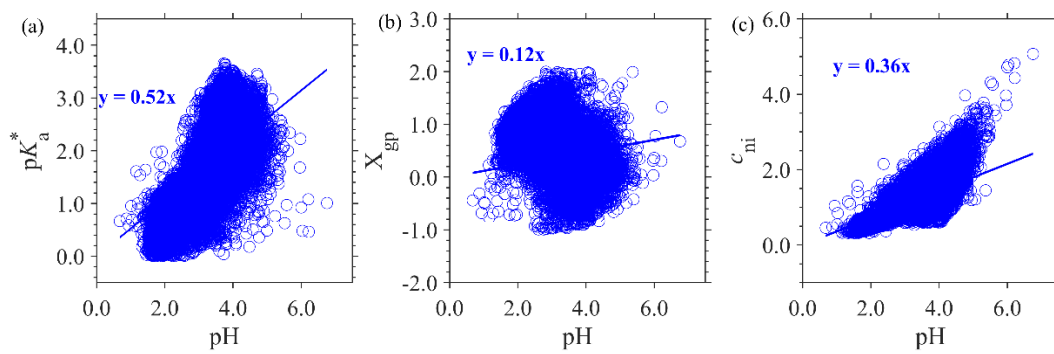


Figure S1: Comparisons of predicted and measured (a) NH₃, (b) NH₄⁺, (c) NO₃⁻, and (d) HNO₃ concentrations in Changzhou during 2018-2023.



95 **Figure S2: Top-level decomposition of pH into (a) pK_a^* , (b) X_{gp} and (c) c_{ni} during the sampling period in Changzhou.**

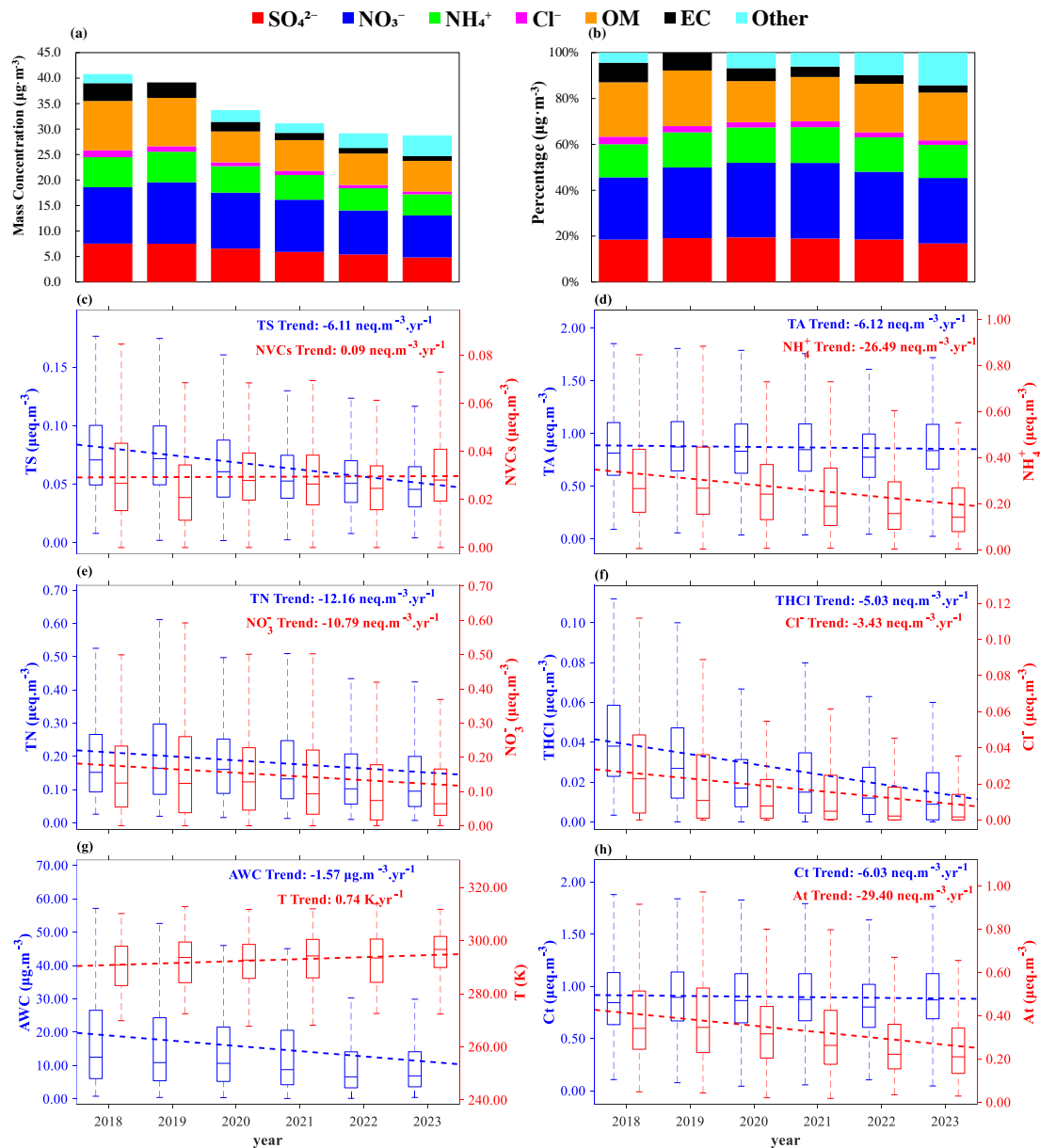


Figure S3: Long-term trends of chemical profiles and meteorology in Changzhou, China from 2018 to 2023.

(a) Mean mass concentrations of chemical profiles, (b) relative percentage of chemical profiles, (c) total sulfate (TS) and non-volatile cations (NVCs), (d) total ammonia (TA) and NH_4^+ , (e) total nitrate (TN) and NO_3^- , (f) total Cl⁻ (THCl) and Cl⁻, (g) AWC and *T*, (h) total cations (*C_t*) and total anions (*A_t*).

100

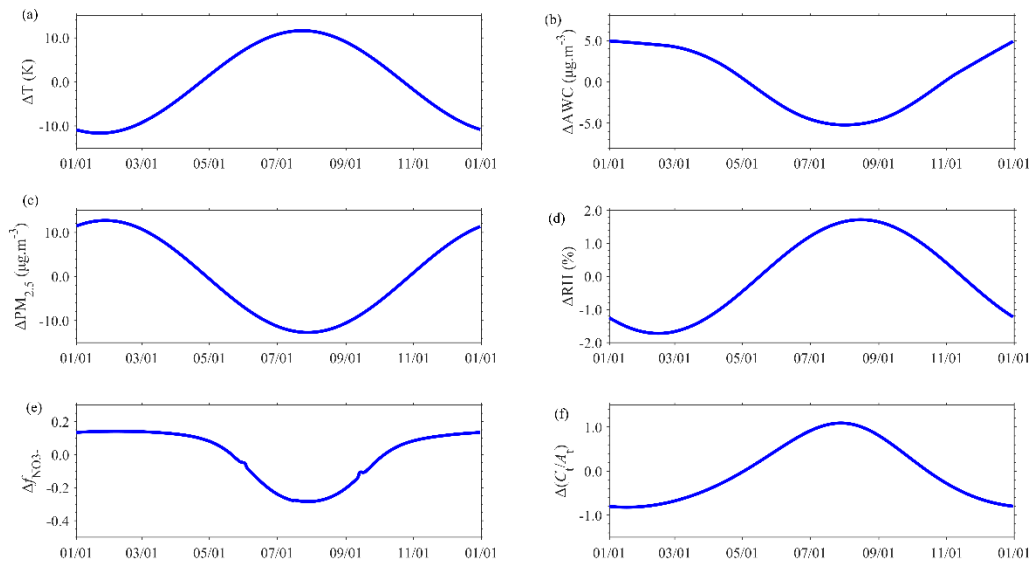


Figure S4: Seasonal variations of (a) T , (b) AWC, (c) $PM_{2.5}$, (d) RH, (e) f_{NO_3} - and (f) C_i/A_i .

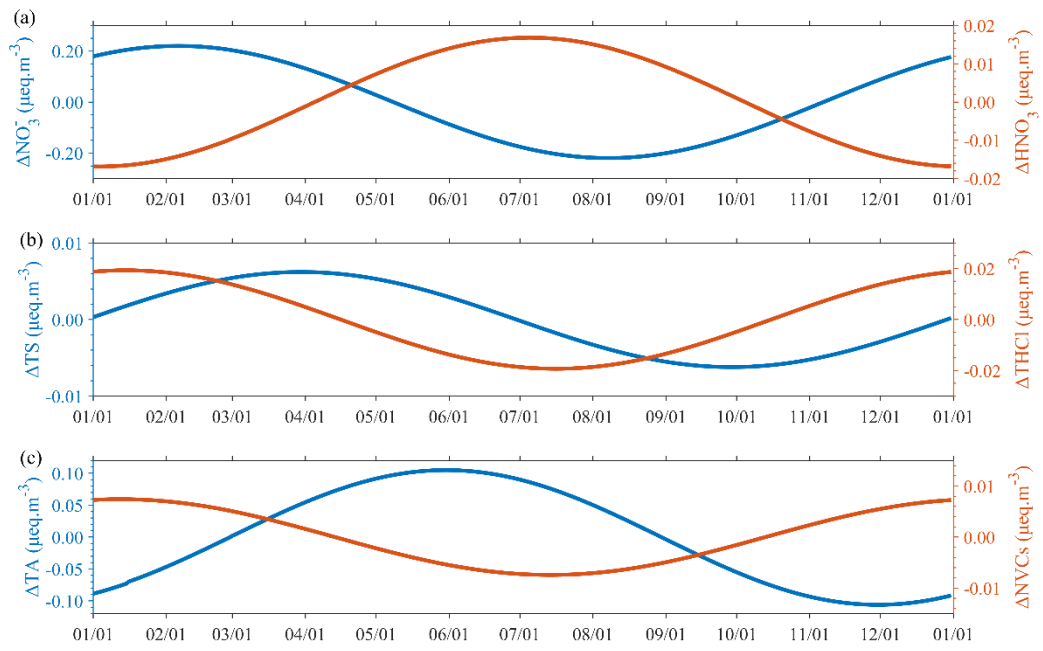
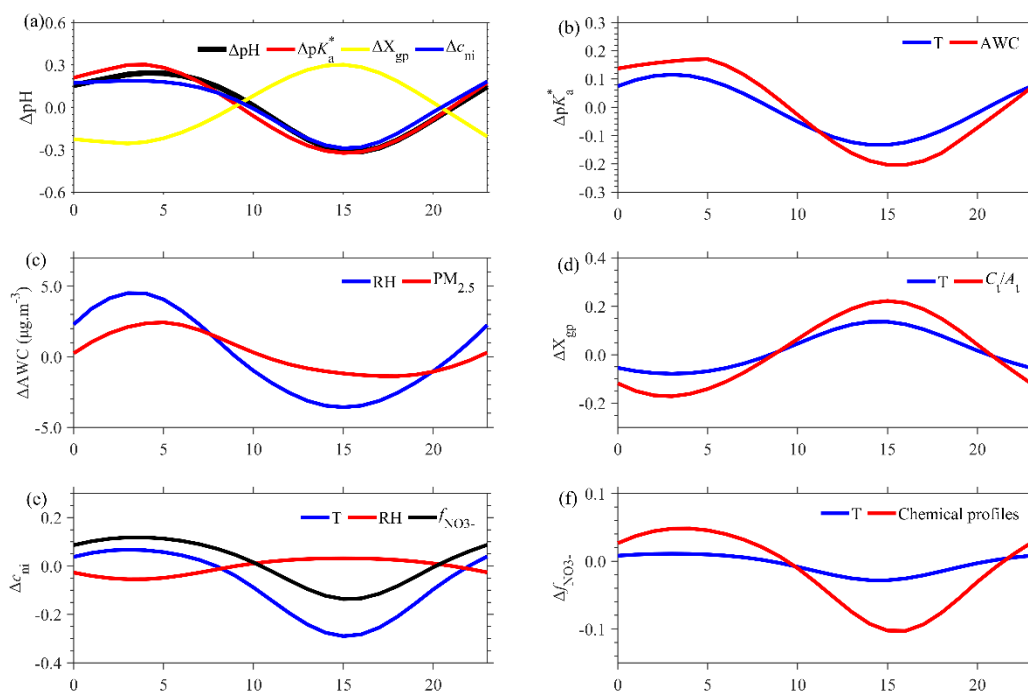


Figure S5: Seasonal variations of (a) NO_3^- and HNO_3 , (b) TSS and THCl , (c) TA and NVCs .



110 **Figure S6: Influencing factors of the diurnal variations of aerosol pH.** (a) The 1st level decomposition into pK_a^* , X_{gp} and c_{ni} . (b)-(f) Further investigation of the influencing factors of (b) pK_a^* due to T and AWC , (c) AWC due to RH and $PM_{2.5}$, (d) X_{gp} due to C/A_t and T , (e) c_{ni} due to RH , T , $f_{NO_3^-}$, and (f) $f_{NO_3^-}$ due to T and chemical profiles.

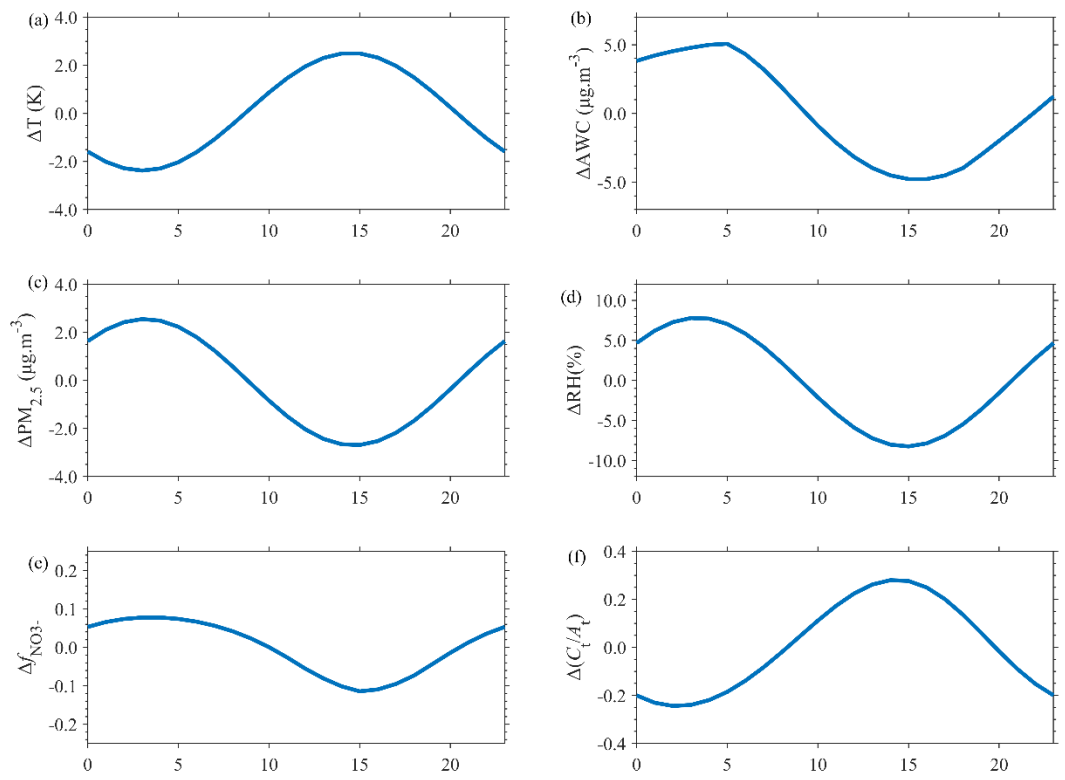


Figure S7: Diurnal cycles of (a) T , (b) AWC , (c) $PM_{2.5}$, (d) RH , (e) $f_{NO_3^-}$ and (f) C_t/A_t .

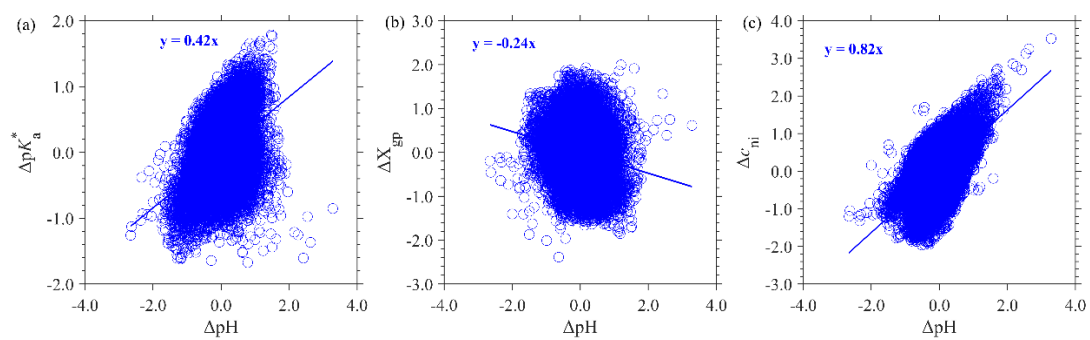


Figure S8: Top-level decomposition of random variations of pH into (a) $\text{p}K_a^*$, (b) X_{gp} and (c) c_{ni} .

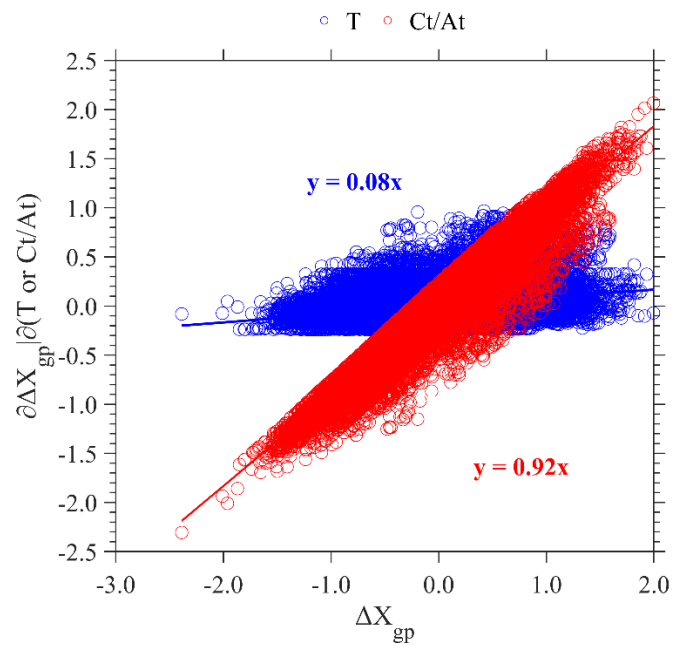
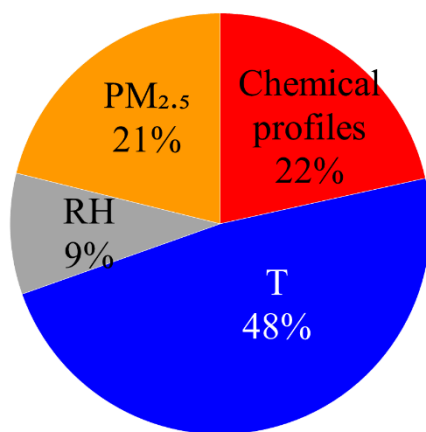


Figure S9: Random variations of X_{gp} due to T and Ct/At .



120

Figure S10: Overall quantitative contribution of *T*, chemical profiles, PM_{2.5} and RH to aerosol pH.

References

- Anderson, T. W.: The statistical analysis of time series, John Wiley & Sons, 2011.
- 125 Wei, W. W. S.: The Oxford Handbook of Quantitative Methods, Vol. 2: Statistical Analysis, Oxford University Press, <https://doi.org/10.1093/oxfordhb/9780199934898.001.0001>, 2013.
- Zheng, G., Su, H., Wang, S., Pozzer, A., and Cheng, Y.: Impact of non-ideality on reconstructing spatial and temporal variations in aerosol acidity with multiphase buffer theory, *Atmos. Chem. Phys.*, 22, 47–63, <https://doi.org/10.5194/acp-22-47-2022>, 2022.
- 130 Zheng, G., Su, H., Wan, R., Duan, X., and Cheng, Y.: Rising Alkali-to-Acid Ratios in the Atmosphere May Correspond to Increased Aerosol Acidity, *Environ. Sci. Technol.*, <https://doi.org/10.1021/acs.est.4c06860>, 2024.